African Journal of Pure & Applied Sciences

ISSN: 2710-0758
DOI 10.33886/ajpas.v3i1.261

Journal homepage: http://journal.ku.ac.ke/index.php/AJPAS

Research Article Open Access

# Positron impact elastic scattering by calcium atom using first order distorted wave born approximation with a complex potential

**Wechuli W. B.[1], Linturi J. M.[2], Kariuki P. K.[1*]**

[1,1*]Department of Physics, Kenyatta University; P.O. Box, 43844–0100, Nairobi, Kenya.
[2] Department of Physical Sciences, South Eastern Kenya University; P.O. Box, 170–90200, Kitui, Kenya.

[1*]Corresponding Author's Email: benardwakhu@gmail.com

**Received: 5th December 2021 / Accepted: 2nd March 2022 / Published online: 1st June 2022**

**How to Cite:**
Wechuli, W., Linturi, J., & Kariuki, P. (2022). Positron impact elastic scattering by calcium atom using first order distorted wave born approximation with a complex potential. *African Journal of Pure and Applied Sciences*, *3*(1), 177-184. https://doi.org/10.33886/ajpas.v3i1.261

## ABSTRACT

Precise positron scattering cross section data are essential for the development of a wide range of technological fields such as astrophysics, plasma sciences, material sciences and bio-medicine. Thus, lack of complete agreement among the available theoretical data, unavailability of experimental data and the first-order distorted wave born approximation with a complex potential at impact energy range 10-200 eV not having been utilized in such a study; are the reasons that informed this investigation. After formulating the complex potential, with positronium formation channel proficiently incorporated, the radial equation was solved numerically. The extracted phase shifts were used to compute the transition matrix. The Roothaan-Hartree-Fock ground state wavefunctions of calcium were utilized in evaluation of the distorting potential and the transition matrix. The transition matrix was then used to determine the differential cross sections while the optical theorem was used to compute total cross sections. With only static potential, the present distorted wave Born approximation and optical potential models yield results that are in close agreement while the effect of positronium formation channel on the cross sections is insignificant at impact energies beyond 150 eV.

**Keywords:** Positron scattering, Cross sections, Positronium, Distorted wave born approximation.

## INTRODUCTION

The concept of elastic scattering of projectiles by atomic targets is crucial to comprehending the convoluted projectile-atom interaction and collision dynamics. According to the Charge, Parity and Time (CPT) theorem, the positron is the electron's antimatter particle. In comparison to electrons, positron scattering is regarded as an alternative means of obtaining information about atomic structures and to examine phenomena such as the Fermi surface of metal and nano-precipitates in solids (Nidhi *et al.*, 2017) and references therein. Further, positron scattering cross section data is essential for the development of various technological fields; for example, astrophysics (Murphy and Share, 2005), plasma sciences (Amour and Tribeche, 2015), material sciences (Hao *et al.*, 2009; Zhang *et al.*, 2010) and bio-medicine (Jan *et al.*, 2004; Fei and Ryoko, 2009). Additionally, positron cross sections are used as input data in some modeling software such as PENELOP (Baro *et al.*, 1995).

Little work has been done on positron-calcium collisions because experimental progress has been stymied by the difficulty in separating distinct partial cross sections as well as obtaining a low-energy monochromatic positron source (Singh *et al.*, 2018). Regrettably, theories are not well developed due to the problem's two-center nature, which necessitates substantial computer resources. The complexity of the equations to be solved in atomic collisions calls for use of approximation methods even when the required wavefunctions are entirely and precisely known. Without loss of generality, there exist three theoretical approaches to computing positron-atom cross sections, that is, use of *ab initio* calculations, working with model potentials and the semi-empirical procedures.

The Harris method employed by Kurtz and Jordan

(1981) as well as the Optical Potential (OP) method of Khare *et al.* (1985) and the Relativistic Polarized Orbital approximation method of Szmytkowski (1993) utilized a real potential hence did not account for absorption effects. Raizada and Baluja (1996) used OP method with a complex potential but the empirical factor they chose to approximately account for positronium formation in their total cross section does not work well to show such behavior as considered herein this study. Singh *et al.* (2018) used OP method with a complex potential that utilized the Staszewska *et al.* (1984) absorption potential which is known to overestimate the flux loss to the electronic excited states for large-angle scattering at high incident energies. The distorted wave born approximation (DWBA) approach has been applied in this research. Further, the Staszewska *et al.* (1984) absorption potential was modified to effectively describe absorption effects while positronium (Ps) formation was accounted for by use of the Chiari *et al.* (2012) model.

## THEORETICAL METHODOLOGY

The projectile considered in this study is distinguishable from atomic and molecular electrons. Consequently, the model potential does not include the exchange potential as required by the Pauli exclusion principle for indistinguishable particles. The interaction potential has been taken in an approximate form and represented by a local, energy-dependent, complex and rotationally invariant potential:

$$V_{opt}\left(r,\mathrm{E}\right)=V_{st}\left(r\right)+V_{pol}\left(r,\mathrm{E}\right)+iV_{abs}\left(r,\mathrm{E}\right) \tag{1}$$

where $V_{st}\left(r\right)$, $V_{pol}\left(r,\mathrm{E}\right)$ and $V_{abs}\left(r,\mathrm{E}\right)$ are respectively the static, polarization and absorption potentials. Because the static interaction with the atom in positron scattering is repulsive, the positron infrequently penetrates deep into the target's charge cloud. The local static potential utilized in this study is similar to the Hartree potential and is given by:

$$V_{st}\left(r\right)=\frac{\mathrm{Z}}{r}-\sum_{n_a l_a}2\left(2l_a+1\right)\int_0^{\infty}dr'\frac{{P_{n_a l_a}}^2\left(r'\right)}{r_>} \tag{2}$$

where $\mathrm{Z}=20$ is the atomic number of the target atom, $r$ is the radial distance, $r_>$ denotes the greater of $r'$ and $P_{n_a l_a}$ are the radial wavefunctions of the electrons of the target atom (Bunge *et al.*, 1993).

As the charged projectile nears target, the target's charge cloud is distorted, resulting in a dipole (or multipole) moment that interacts with the impact particle generating the attractive polarization potential. The Khare *et al.* (1985) polarization potential, given by equation (3) hereunder, was used in this investigation.

$$V_{pol}\left(r,E\right)=-\frac{1}{2}\left\{\frac{\alpha_d r^2}{\left(r^2+d^2\right)^3}+\frac{\alpha_q r^4}{\left(r^2+d^2\right)^5}\right\} \tag{3}$$

where the cutoff radius, $d$, that prevents $V_{pol}\left(r,\mathrm{E}\right)$ from diverging at $r=0$ is given by $d=\frac{3}{4}\left(\frac{1.78}{\Delta}\right)^{\frac{1}{2}}$, $\alpha_d=168.71$ (experimental results of Miller and Bederson, 1976), and $\alpha_q=3356.96$ (Sen and Schmidt, 1981) and $\Delta=0.14635$ atomic units; are respectively the dipole polarizability, quadrupole polarizability and the mean excitation energy.

The total loss of dispersed flux into all permissible channels of inelastic processes such as electronic excitation, direct ionization and Ps-formation is accounted for by the imaginary part of the complex potential. In this investigation, we employed a modified version of Staszewska *et al.* (1984) model potential:

$$V_{abs}\left(r,\mathrm{E}\right)=\frac{V_{\mathrm{I}}\left(r,\mathrm{E}\right)}{k} \tag{4}$$

where $k=\sqrt{2\mathrm{E}}$ is the magnitude of the momentum vector of the incident positron of energy $\mathrm{E}$, $V_{\mathrm{I}}\left(r,\mathrm{E}\right)=-T_{loc}\left(r,\mathrm{E}\right)\rho\left(r\right)\sigma_b$ is, for positron scattering, the absorption potential of Staszewska *et al.* (1984) in which $\rho\left(r\right)=\sum_{nl_a}2\left(2l_a+1\right)\frac{P_{n_a l_a}}{4\pi r^2}$ is the electronic charge density of the target atom, $\mathrm{T}_{loc}\left(r,\mathrm{E}\right)=\left[2\left(\mathrm{E}-V_{st}\left(r\right)\right)\right]^{\frac{1}{2}}$ is the local kinetic energy of the incident positron and $\sigma_b$ is the average binary collision cross section (Staszewska *et al.*, 1984). The inelastic threshold of the target atom, $\Delta_{\mathrm{I}}$, determines the threshold below which $V_{abs}\left(r,\mathrm{E}\right)=0$. Because of Ps-formation, determining $\Delta_{\mathrm{I}}$ is a difficult process in positron scattering. Ps-formation channel cannot be incorporated into equation (4) as a separate elastic event because it cannot be explained in terms of binary collisions. In this research, the Chiari *et al.* (2012) absorption threshold, given as equation (5) hereunder, was adopted:

$$\Delta_{\mathrm{I}}=\Delta_e-\left(\Delta_e\right)\exp\left\{\frac{-\left(\mathrm{E}\right)}{\mathrm{E}_m}\right\} \tag{5}$$

where $\Delta_e=2.939$ eV (Sansonetti *et al.*, 2005) is the lowest electronic excitation energy of the atomic target (Calcium), $\mathrm{E}$ is the energy of incident positron and $\mathrm{E}_m=10$ eV is the energy at which the inelastic cross section reaches its maximum without taking Ps-formation into account. The projectile considered herein this study is distinguishable

from atomic electrons thus the DWBA transition matrix is evaluated only in terms of direct matrix element whose terms are given in computation form [equations (6) and (7)] as:

$$T_{i0}^{D1} = -\frac{1}{4\pi^2}\frac{1}{k}\sum_{l=0}^{\infty}(2l+1)e^{i\delta_l}\sin\delta_l P_l(\cos\theta) \quad (6)$$

$$T_{i0}^{D2} = \frac{1}{2\pi^2}\frac{1}{k^2}\sum_{l=0}^{\infty}(2l+1)e^{i2\delta_l}\left\{\int_0^{\infty} dr\chi_l(k,r)\overline{V}(r,E)\chi_l(k,r)\right\}P_l(\cos\theta) \quad (7)$$

where $P_l(\cos\theta)$ are Legendre polynomials of order $l$, $\cos\theta = \hat{k}_0.\hat{k}_i$ with $k_0\,(k_i)$ being the initial (final) momentum and the residual potential $\overline{V}(r,E) = -\left[V_{pol}(r,E) + iV_{abs}(r,E)\right]$. The differential cross section (DCS) is given by:

$$\frac{d\sigma}{d\Omega} = (2\pi)^4\frac{k_i}{k_0}|T_{i0}|^2 \quad (8)$$

where $T_{i0} = T_{i0}^{D1} + T_{i0}^{D2}$ is the transition matrix. For elastic scattering using a spherically symmetric potential as applied in this research, the transition matrix of OP model contains the element given by equation (6) only while in the DWBA model, it contains both equations (6) and (7). The total cross section, $(\sigma_T)$, is given by the optical theorem:

$$\sigma_T = -\left(\frac{2}{k_0}\right)(2\pi)^3\,\mathrm{Im}\,T_{00} \quad (9)$$

where $k_0$ is the scattered positron's momentum and $T_{00}$ is the T-matrix for $\theta = 0$. The absorption cross section is given by:

$$\sigma_{abs} = \frac{\pi}{k^2}\sum_{l=0}^{\infty}(2l+1)\left(1-e^{-4\beta_l}\right) \quad (10)$$

where $\beta_l = \ln\left(1-\frac{1}{k\cos\alpha_l}I\right)$ is the imaginary part of the complex phase shift, $\delta_l$, evaluated in terms of the real part, $\alpha_l$, and the integral $I = \int_0^{\infty} dr' f_l(kr')V_{abs}(r')w_l(k,r')$ which contains the imaginary part of the interaction potential, the regular Ricatti-Bessel function , $f_l(kr')$, and the real part of the distorted wave $\chi_l(k,r) = w_l(k,r) + iz_l(k,r)$. The total elastic cross section for both OP and DWBA methods were obtained using the equation:

$$\sigma_{el} = \sigma_T - \sigma_{abs} \quad (11)$$

## NUMERICAL PROCEDURE

We have utilized the modified PDWBA_Ca program, written in C language, to theoretically determine positron-calcium DCS, TCS (elastic) and TCS (elastic and inelastic) at impact energy $10 \le E \le 200$ eV. For a rotationally invariant potential, $V_{opt}(r,E)$, the scattering process is symmetric about the direction of the incident positron. The solution, $\chi_l(k,r)$, is generated by the radial Schrödinger equation (in atomic units):

$$\left[\frac{d^2}{dr^2} - \frac{l(2l+1)}{r^2} - V_{opt}(r,E) + k^2\right]\chi_l(k,r) \quad (12)$$

where $k$ is the momentum wave vector of the projectile positron and $l$ is the angular momentum quantum number. For $l \le 7$, the Numerov's method (Madison and Bartschat, 1996) was used to numerically solve radial Schrödinger equation (12) using the potential in equation (1) and the phase shifts, $\delta_l$, determined from:

$$\tan\delta_l = -\frac{kf_l' - \gamma f_l}{kg_l' - \gamma g_l} \quad (13)$$

where $f_l\,(g_l)$ is the regular (irregular) Ricatti-Bessel functions while $\gamma_l = \chi_l^{-1}\left(\frac{d\chi_l}{dr}\right)$, $f_l' = \frac{df_l}{d\rho}$, $g_l' = \frac{dg_l}{d\rho}$ and $\rho = kr$. For $l \ge 7$, extraction of phase shifts using equation (13) from un-normalized radial wavefunctions is prone to errors. Thus, the integral equation (Mertzbacher, 1970) associated with the radial differential equation (12) was solved iteratively and the phase shifts obtained as:

$$\tan\delta_l = -\frac{1}{k}\int_0^{\infty} dr' f_l(kr')U_{opt}(r')\chi_l(k,r) \quad (14)$$

where:

$$\chi_l(k,r) = \frac{\chi_l(k,r)}{\cos\delta_l} \quad (15)$$

The multipole integral in the static potential, equation (2) was expanded as:

$$I = \int_0^{\infty} dr' \frac{P_{n_a l_a}^2(r')}{r_>} = \frac{1}{r}\int_0^{r} dr' P_{n_a l_a}^2(r') + \int_r^{\infty} dr' \frac{P_{n_a l_a}^2(r')}{r'} \quad (16)$$

Both the forward and backward integrals in equation (16) were evaluated using the five-point quadrature rule (Fischer *et al.*, 1997) and the Simpson's ⅓ rule (Press *et al.*, 1992) utilized at the ends of integration range.

## RESULTS AND DISCUSSION

### Present and Khare *et al.* (1985) OP Models

The present OP DCS [in atomic units (a.u)] results, for static potential and static-polarization potentials, are respectively denoted by OP_S and OP_SP while the Khare *et al.* (1985) results are respectively denoted by OP_SK and OP_SPK. At all of the impact energies investigated herein, the present DCS results of OP_S and the theoretical results of OP_SK demonstrate good numerical agreement with a deviation of $\pm 0.25\%$ [Figures 1(a), 1(b) and 1(c)]. At 10 eV [Figure 1(a)], OP _SP DCS and OP_SPK results agree within $1.3\%$. The difference in results is attributable to use of different values of $d$, the parameter that avoids singularity at $r = 0$ in equation (3). For incident energies $\mathrm{E} > 3.56\Delta$, Khare *et al.* (1985) used $d = \frac{3k}{8\Delta}$. In these models, polarization potential did raise DCS values at low scattering angles and further introduced a local minimum at $40^{\circ}$.

At 40 eV [Figure 1(b)], polarization potential increases the DCS values at scattering angles $\theta \leq 10^{\circ}$. The minimum (maximum) represents the direction in which the projectile is least (most) likely to be deflected. For the reason stated herein above, the present OP_SP results slightly overestimate the OP_SPK results at scattering angles $\theta \leq 85^{\circ}$. At 75 eV [Figure 1(c)], inclusion of polarization potential leads to increase in DCS values at scattering angles $\theta \leq 10^{\circ}$; though the values have generally reduced, compared to the results at 10 eV, since the contribution of the quadrupole term in the polarization potential decreases with increase of the projectile's impact energy. Accordingly, the results from the two models agrees within $2.1\%$.

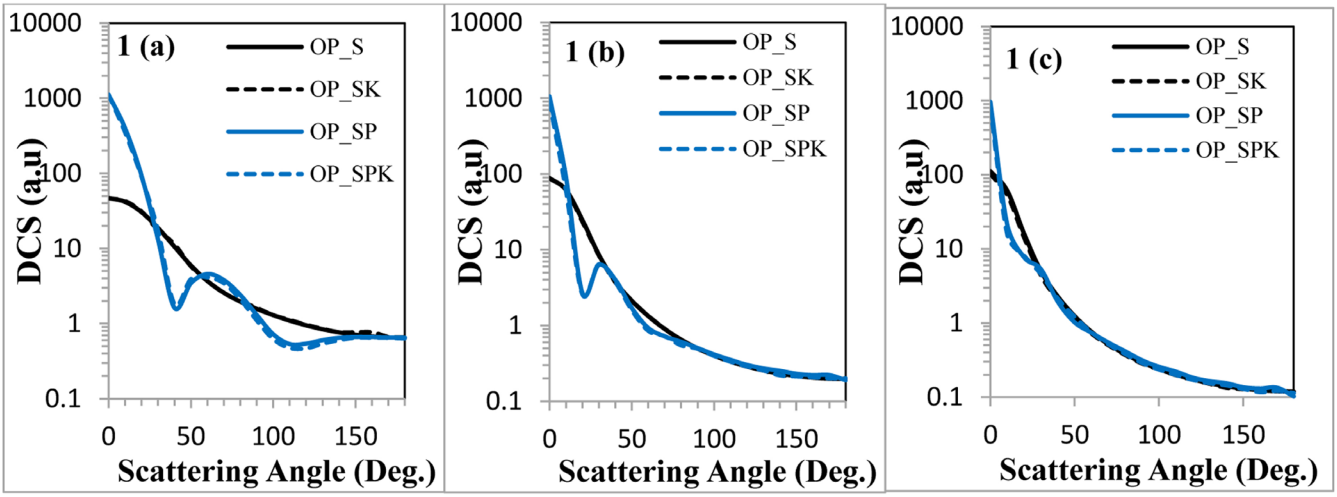


**Figure 1(a):** Differential cross sections for positron-calcium atom elastic scattering at 10 eV: OP_S –present results with static only, OP_SP –present results with static and polarization, OP_SK – Khare *et al.* results with static only, OP_SPK - Khare *et al.* results with static and polarization. **Figures 1(b) and 1(c):** Same as in **figure 1(a)** but respectively at 40 eV and 75 eV

### OP and DWBA Methods

The present OP and DWBA DCS results are respectively represented by OP_S and DWBA_S (for static potential); OP_SP and DWBA_SP (for static-polarization potentials). OP and DWBA complex potential with (without) positronium results are respectively denoted by OP_SPA-Ps and DWBA_SPA-Ps (OP_SPA and DWBA_SPA). The present DCS results of OP_S and DWBA_S are in exact agreement at all the positron-impact energies considered in this study. The exact agreement is due to the fact that when $V_{opt}(r, \mathrm{E}) = V_{st}(r)$, the second direct term in the DWBA T-matrix element, $\mathrm{T}_{i0}{}^{D2}$, [equation (7)] vanishes. Further, since the positron is quantum mechanically distinguishable from the target electrons, the exchange element in DWBA T-matrix is dropped. Consequently, DWBA is equal to OP method.

At 10 eV [Figure 2(a)], although the OP _SP DCS results exceed those of DWBA_SP by about $4.3\%$ for scattering angle $0^{\circ} \leq \theta \leq 40^{\circ}$. Beyond the position of local minimum, these models yield results that generally agree within $1.6\%$. For positron scattering, the repulsive-static and the attractive-polarization potentials tend to cancel each other. Thus, the effect of the residual potential in equation (7), which contains the repulsive-attractive effects of static-polarization potentials, is to lower the DWBA DCS values at small scattering angles where polarization potential has greater impact on the scattering cross sections. As explained earlier, at all the potentials investigated in this study, the absorption potential slightly lowers the DCS values. There is very good agreement between the OP_SPA and DWBA_SPA DCSs, with a deviation of $\pm 0.67\%$, which corroborates the fact that the effect of the second direct term [equation (7)] vanishes as the distorting potential becomes more complete.

Incorporating positronium formation [equation (5)] into the absorption potential [equation (4)] leads to a slight decrease in the DCS values at the given impact energies up to around 150 eV for both OP_SPA-Ps and DWBA_SPA-Ps. Beyond 150 eV, Ps-formation has no effect on the cross-sections.

At 15 eV and 20 eV, there is a marked good agreement between OP_SP and DWBA_SP with a deviation of $\pm 2.2\%$. The local minimum occurs at $\theta = 30^{\circ}$. At these impact energies, the polarization potential increases the DCS results at small scattering angles (though not as much as in the case of 10 eV) since this is potential experienced by projectile particles moving far away from the target. Thus, higher DCS values at low scattering angles implies more positrons deviate from their initial straight trajectories through small angles.

At 40 eV, the local minimum occurs at $20^{\circ}$. The current OP_SP and DWBA_SP results are in conformity since the agreement is within $0.38\%$. This implies a decrease in the effect of equation (7) on the DWBA DCSs. At 75 eV, inclusion of polarization potential has led to increase in DCS values at scattering angles $\theta \leq 10^{\circ}$; though the values have generally reduced since the contribution of the quadrupole term in the polarization potential decreases with increase of the projectile's impact energy. There is good agreement between the OP_SP and DWBA_SP.

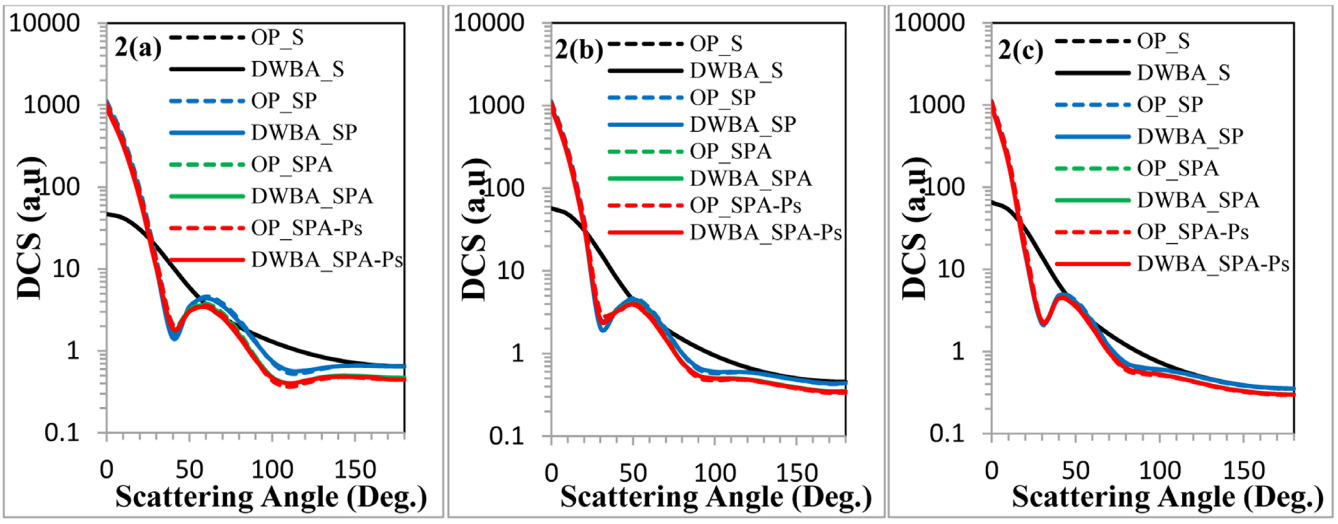


**Figure 2(a):** Differential cross sections for positron-calcium atom elastic scattering at 10 eV: DWBA_S and OP_S – present results with static only; DWBA_SP and OP_SP –present results with static and polarization; DWBA_SPA and OP_SPA- present results with static, polarization and absorption; DWBA_SPA-Ps and OP_SPA-Ps – present results with complex potential and positronium. **Figures 2(b) and 2(c):** Same as in **figure 2(a)** but respectively at **15 eV** and **20 eV**

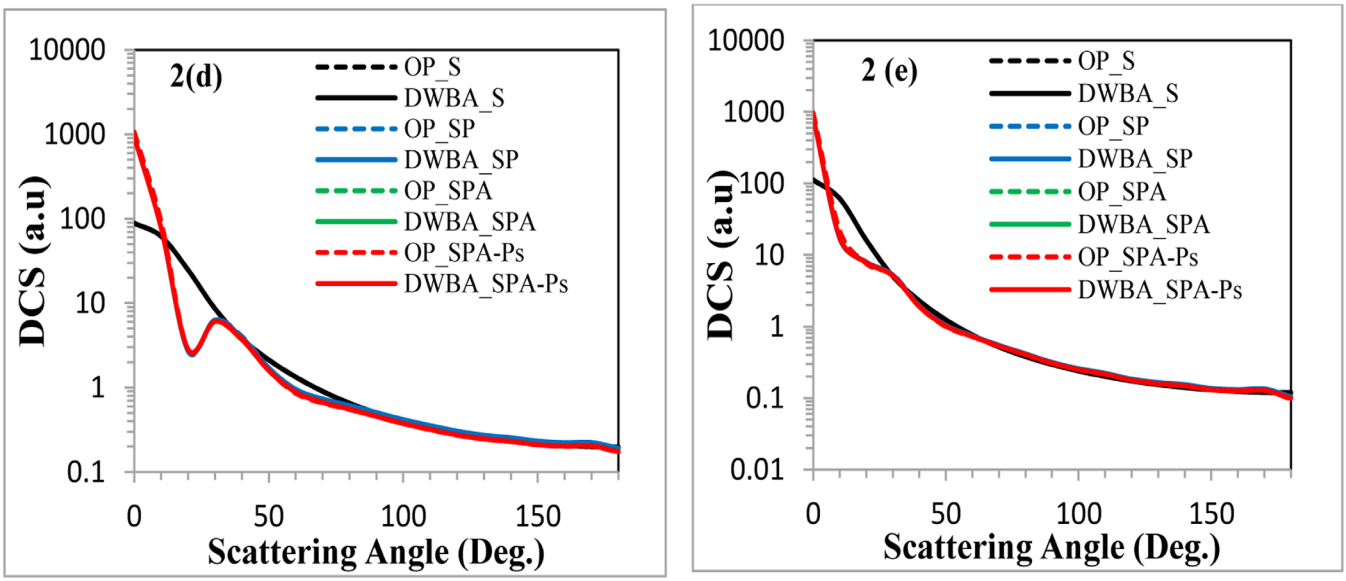


**Figures 2(d) and 2(e):** Same as in **figure 2(a)** but respectively at **40 eV** and **75 eV**

At 100 eV and 150 eV - both qualitative and numerical agreement between OP_SP and DWBA_SP is excellent with minor differences within $0.3\%$ at the local minimum. This confirms the insignificance of the second direct term [equation (7)] in the DWBA T-matrix element on the DCS values with increase in positron-impact energy. Noting that the residual potential in equation (7) is due to the energy-dependent polarization, then the DCS agreement means that the polarization effect decreases with increase in impact energy and is expected to vanish at very high energies. At 100 eV, the present positron-calcium DCS results, that is, OP_P_SPA-Ps and DWBA_P_SPA-Ps are in excellent agreement with a deviation of $\pm 0.16\%$. Similarly, the present electron-calcium (OP_E_SPA and DWBA_E_SPA) results agree within $0.16\%$. This implies the insignificance of the second element of the direct term of the T-matrix in DWBA as the distorting potential becomes complete. Although the exchange potential as well as the exchange element of the T-matrix (for DWBA method) were excluded in the present theoretical formalism, our findings are generally consistent with Milisavljevic *et al.* (2005) experimental results within $0.77\%$ for $\theta \leq 50^{o}$. For $\theta \geq 60^{o}$, the present absorption potential did not adequately account for loss of flux into inelastic channels hence the difference with experimental results. At small scattering angles, the current electron results often exceed the current positron results since for electrons; static and polarization potentials are both attractive and add up while for positrons static is repulsive and tend to cancel the attractive effects of polarization potential.

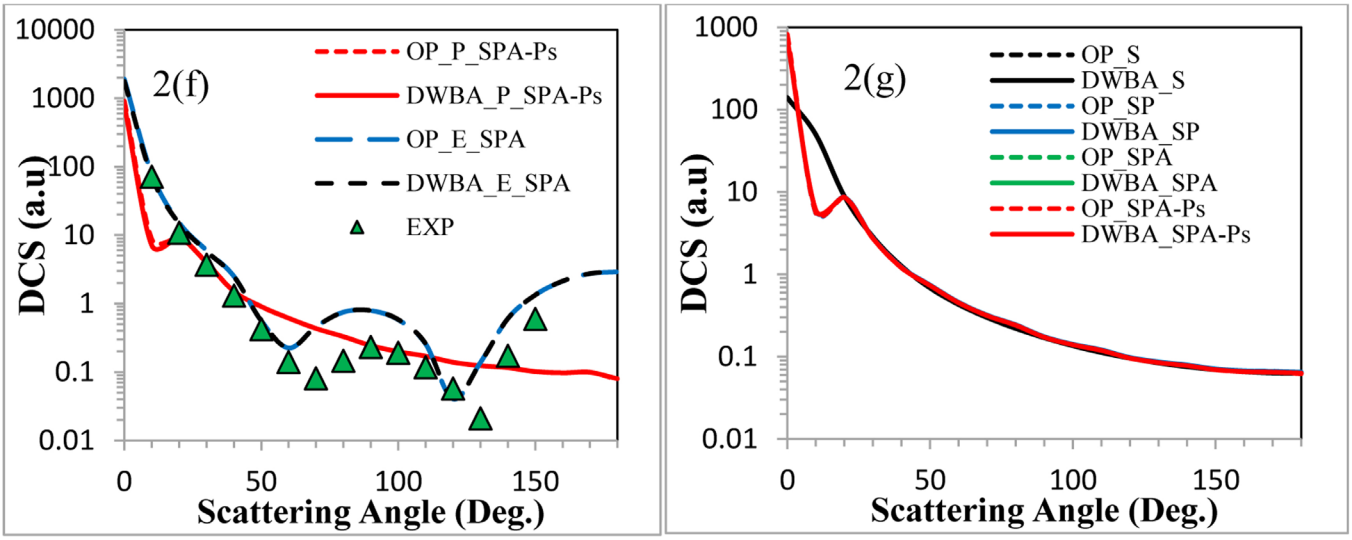


**Figure 2(f):** DCS at 100 eV: **Theory**: OP_P_SPA-Ps and DWBA_P_SPA-Ps – present positron-calcium elastic scattering differential cross sections with a complex potential and positronium; OP_E_SPA and DWBA_E_SPA – present electron-calcium DCS with complex potential but no exchange; EXP – Electron-calcium experimental data of Milisavljevic *et al.* (2005) while **figure 2(g)** is same as in **figure 2(a)** but **150 eV**

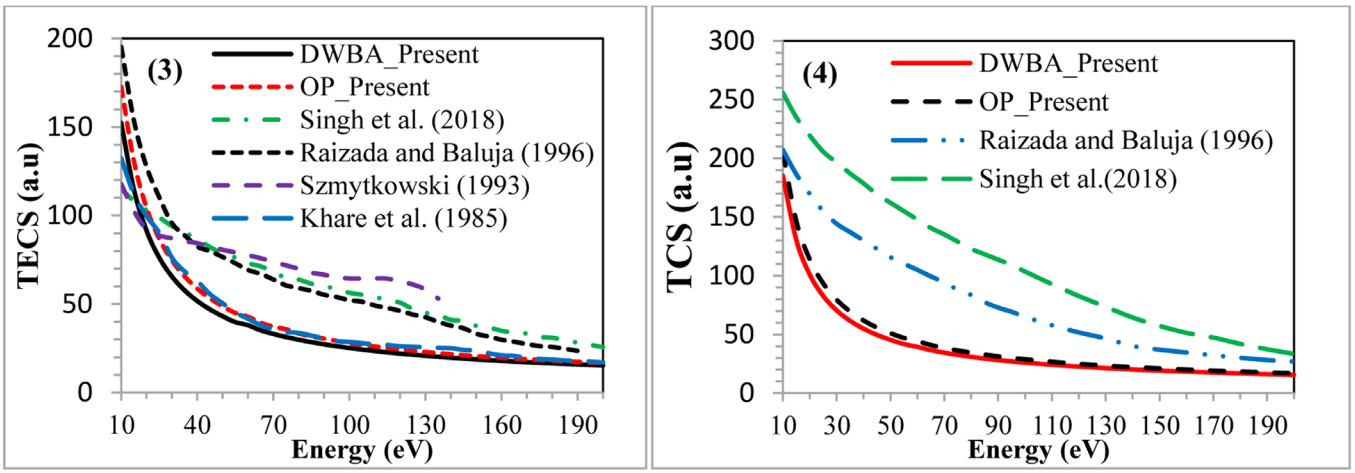


**Figures 3 and 4:** Show respectively the Total Elastic Cross Section (TECS) and Total Elastic and Inelastic (TCS) Cross Section for positron-calcium atom scattering at impact energy $10 \leq E \leq 200$ eV

### Total Elastic Cross Section

**Figure 3:** The current dataset compares quite well with the curves of Khare *et al.* (1985) within $\pm 4.6\%$ for OP at $E \geq 20$ eV and $6.2\%$ for DWBA at $E \geq 10$ eV. The dataset of Singh *et al.* (2018) and Raizada and Baluja (1996) averagely overestimate the present data by $10.89\%$ and $10.03\%$ respectively at $E \leq 130$ eV due to use of different distortion potentials. Beyond 130 eV, the cross sections tend to merge since at such high impact energies, the cross sections do not depend on the interaction potential as much as they do on the projectile's kinetic energy. At impact energies $E \leq 20$ eV, the present DWBA results exceeds the data of Szmytkowski (1993) by ; $11.1\%$. Beyond this energy, the data of Szmytkowski (1993) deviates by $20.07\%$ from the present data and shows higher values with diverging nature due to the rise in elastic cross sections. Save for the data of Szmytkowski (1993), the rest decrease with increase in impact energy implying decrease in probability of scattering due to the reduced projectile-target interaction time.

### Total Cross Section

**Figure 4**: The shape and structure of the present OP and DWBA, Singh *et al.* (2018) and Raizada and Baluja (1996), each with a complex potential that incorporates positronium channel, exhibit same trend; that is, the cross sections reduce with increase in impact energy. However, on average, the present TCS results have less magnitude of cross sections by $24.3\%$ and $37.6\%$ respectively below the curves of Raizada and Baluja (1996) and Singh *et al.* (2018). Raizada and Baluja (1996) used the empirical factor, $\left[(kr)^{-1}\right]^{\frac{1}{2}}$, to approximately account for Ps-formation. From their results, for beryllium (Be), TCS (elastic) = TCS (elastic and inelastic) $= 15$ square angstrom at 10 eV. This suggests that the inelastic cross section is zero which is in fact incorrect since the Ps-formation threshold for Be ; $2.523$ eV; thus, the inelastic cross section should have significant value at impact energy $E = 10$ eV. Therefore, the difference between Raizada and Baluja's results and our present data is due to their inadequate handling of Ps-formation and use of Staszewska *et al.* (1984) absorption potential which was also utilized by Singh *et al.* (2018) yet it is known to overestimate TCSs.

## CONCLUSION

We have applied the DWBA and OP methods with a complex potential to calculate differential, total (elastic) and total (elastic and inelastic) cross sections. With a complex potential that incorporates positronium formation channel, the effect of the second order terms of the complex potential that constitutes the residual potential used in the second element of the direct T-matrix is negligible hence exact agreement between DWBA and OP differential cross sections.

The positronium formation channel slightly increases the total cross sections at low impact energies up to about 150 eV. Its effect on the cross sections beyond 150 eV is insignificant.

The position of the local minimum in DCS shifts toward forward scattering angles with increasing projectile-target impact energy; a behavior attributed to the energy-dependent polarization potential since the polarization effects are expected to vanish at very incidence energies. Since positronium formation channel of calcium is open from the onset, the observed monotonous decreasing nature of total (elastic and inelastic) cross sections is evidence for high inelastic channels at low energies. At high impact energies $(E \geq 160)$, the predicted cross sections tend to converge. This behavior conforms to first Born approximation. To the best of our knowledge, there are no experimental results for positron-calcium scattering. We therefore hope that our results will be useful for comparison with future experimental outcome.

## REFERENCES


Amour, R., and Tribeche, M. (2015). *Effects of electron suprathermality and positron density on ion acoustic dressed solitons in an electron-positron-ion plasma*. IEEE International Conference on Sciences (ICOPS).

Baro, J., Sempau, J., Fernandez-Varea, J. M., and Salvat, F. (1995). PENELOPE: an algorithm for Monte Carlo simulation of the penetration and energy loss of electrons and positrons in matter. *Nuclear Instruments and Methods, 100*(1), 31–46.

Bunge, C. F., Barrientos, J. A., and Bunge, A.V. (1993). Roothaan-Hartree-Fock Ground State Atomic wavefunctions: Slater-Type-Orbit Expansions and Expectation Values for $Z = 2 - 54$. *Atomic Data and Nuclear Data Tables, 53*, 113–401.

Chiari, L., Zecca, A., Girardi, S., Trainotti, E., Blanco, F., McEachran, R. P., and Brunger, M. J. (2012). Positron scattering from $O_2$. *Journal of Physics B: Atomic, Molecular and Optical Physics*, *45* (21), 1–9, 215206. URL https://dx.doi.org/10.1088/0953-4075/45/21/215206.

Fei, G., and Ryoko, Y. (2009). An effective scatter correction method based on single scatter simulation for a 3D whole-body PET scanner *Chinese Physics B, 18*(7), 1674–1056, 3066-07.

Fischer, C. F., Brange, T., and Jonsson, P. (1997). *Computational atomic structure*. London: Institute of Physics.

Hao, X. P., Zhou, C. L., Wang, B. Y. and Wei, L. (2009). Defects in Si-Rich $SiO_2$ films prepared by radio-

frequency magnetron co-sputtering using variable energy positron annihilation spectroscopy. *Chinese Physics Letters, 27*, 013401.

Jan, S., Santin, G., Strul, D., Staelens, S., Assie, K., Autret, D., …… Morel, C. (2004). GATE: a simulation toolkit for PET and SPECT. *Physics in Medicine and Biology, 49*(19), 4543–4561. URL https://doi.org/10.1088/0031-9155/49/19/007.

Khare, S. P., Kumar, A., and Vijayshri, K. V. (1985). Elastic scattering of electrons and positrons by Ca atom. *Journal of Physics B: Atomic and Molecular Physics*, *18*(9), 1827–1840. URL https://stacks.iop.org/0022-3700/18/i=9/a=016.

Kurtz, H. A., and Jordan, K.D. (1981). Theoretical study of low-energy electron and positron scattering on Be, Mg and Ca. *Journal of Physics B: Atomic and Molecular Physics*, *14*(22), 4361–4372. URL https://stacks.iop.org/0022-3700/14/i=22/a=019.

Madison, D. H., and Bartschat, K. (1996). *The distorted wave method for elastic scattering and atomic excitation. In Computational Atomic Physics.* Ed. K. Bartschat. Springer Verlag, Berlin.

Mertzbacher, E. (1970). *Quantum Mechanics.* New York: John Wiley and Sons Ltd.

Milisavljevic, S., Sevic, D., Chauhan, R. K., Pejcev, V., Filipovic, D. M., Srivastava, R., and Marinkovic, B. P. (2005). Differential and integrated cross sections for the elastic electron scattering by calcium atom. *Journal of Physics B: Atomic, Molecular and Optical Physics*, *38*(2005), 2371–2384. DOI:10.1088/0953-4075/38/14/004.

Miller, T. M., and Bederson, B. (1976). Measurement of the polarizability of calcium. *Physical Review A*, *14,* 1572.

Murphy, R. J., & Share, G. H. (2005). The physics of positron annihilation in the solar atmosphere. *The Astrophysical Journal Supplement Series*, *161*, 495–519.

Nidhi, S., Suvam, S., and Bobby, A. (2017). Positron total scattering cross-sections for alkali atoms. *Journal of Physics B: Atomic, Molecular and Optical Physics*, *51*(2018), 015204. https://doi.org/10.1088/1361-6455/aa949d.

Press, W. H., Teukolsky, S. A., Vetterling, W. T., and Flannery, B. P. (1992). *Numerical recipes in C: The art of scientific computing*. Cambridge: Cambridge University Press.

Raizada, R., and Baluja, K.L. (1996). Positron scattering from alkaline-earth elements. *Pramana*, *47*(1), 87–98. DOI: 10. 1007/BF02847169. URL https://dx.doi.org/10.1007/BF02847169

Sansonetti, J., Martin, W., and Young, S. (2005). *Handbook of basic atomic spectroscopic data*. NIST. URL https://www.nist.gov/pml/handbook-basic-atomic-spectroscopic-data

Sen, K. D., and Schmidt, P. C. (1981). Static dipole and quadrupole polarizabilities of alkaline earth atoms. *International Journal of Quantum Chemistry, 19*(2), 373–376.

Singh, S., Anamika, S., and Bobby, A. (2018). Positron scattering calculations of elastic, total and momentum transfer cross sections for alkaline earth atoms. *International Journal of Mass Spectrometry*, *428*, 22–28. URL https://doi.org/10.1016/j.ijms.2018.02.005.

Staszewska, G., Schwenke, D. W., Thirumalai, D., and Truhlar, D. G. (1984). Quasifree-scattering model for the imaginary part of the optical potential for electron scattering. *Physical Review A*, *28*(1984), 2740–2751. DOI: 10. 1103/PhysRevA. 28. 2740. URL https://link.aps.org/doi/10.1103/PhysRevA.28.2740.

Szmytkowski, R. (1993). Theoretical study of low-energy positron scattering on alkaline-earth atoms in the relativistic polarized orbital approximation. *Journal of Physics II France, 3*(2), 183–189. DOI: 10.1051/jp2:1993120. URL https://doi.org/10.1051/jp2:1993120.

Zhang, S. B., Qi, Y. Y., Qu, Y. Z., Chen, X. J., and Wang, J. G. (2010). Positron impact excitation of hydrogen atoms in Debye plasmas. *Chinese Physics Letters, 27*, 013401.